Journal of Engineering and Applied Sciences 5 (4): 257-263, 2010
ISSN: 1816-949X

Modeling a Non-Ferrous Melting Furnace

O.A. Ighodalo
Department of Mechanical Engineering, Ambrose Alli University, Ekpoma, Nigeria

Abstract: Different types of models are available for purpose of system simulation, modification, optimization and control. The one-dimensional model employed in simulating a non-ferrous melting furnace is presented. The model consists of a governing equation for the combustion chamber and a transient heat conduction equation for the walls and roof. Each furnace component is treated as a one-dimensional conduction medium and the governing equations are solved numerically. The model was tested for the case of melting 3 kg of aluminium charge in a furnace designed for melting non-ferrous metals. From the output of the program, the maximum temperatures obtained at the end of melting for walls and roof, in-furnace average gas temperature (avtg) and stack or exhaust gas were compiled and compared with experimental values. Higher temperature values were obtained when compared with experimental values. The wall temperature simulations are observed to be closely coupled an indication of a uniform temperature distribution within the furnace which was also reflected in the heat flux for the surfaces. The simulations are adjudged comparable with experimental data and the model is thus capable of predicting the key independent variables.

Key words: Furnace modeling, one-dimensioal, simulations, temperature, melting furance, Nigeria

INTRODUCTION

A mathematical model is a set of equations, algebraic or differential which may be used to represent and predict certain phenomena (Szekely, 1988). Such models may be built from basic physical (including mechanical) and chemical laws or by drawing on the analogy of previous research through consideration of some basic physical situations.

Mathematical models may also be built from experiments with scale down physical models. The use of mathematical models thus makes possible the simulation and modification of system behaviour. System optimization and control are other important advantages of using mathematical models. The different model types vary both in their degree of complexity and the information obtained upon their application. According to Khalil (1982) and Baukal *et al.* (2001), three different types exist. These are zero, one, two and three-dimensional models.

In zero-dimensional modeling an overall heat and material balance of the system is done. This type of model does not give any spatial resolution but still gives a reasonable approximation of the overall performance of the system.

One-dimensional modeling considers only one spatial dimension and this greatly simplifies the number of equations, these models may still be fairly complicated and provide many details into the spatial changes of a given parameter. Two and three-dimensional models models allow the determination of the spatial distribution of fluid and heat flow and other properties.

Appropriate approximations of the real situation, leads to the solution of simultaneous partial differential equations which represent the conservation of mass, momentum, energy and species. A melting furnace for non-ferrous metals have been previously developed and tested (Ighodalo and Ajuwa, 2010), the aim of the present research is to present the one-dimensional model employed in simulating the furnace thermal characteristics and the results obtained.

MATERIALS AND METHODS

Description of the furnace: The gas-fired melting furnace has been described by Ighodalo and Ajuwa (2010). The furnace walls are made from refractory castable material and are 110 m thick.

A 10 m thick fibre-glass insulation was sandwiched between the outer face of the refractory walls and the encasing steel which is 1.5 m thick.

The whole frame research is a cubicle box, 700×600 ×600 mm with provisions for a burner hole, a chimney hole, a spout opening and charging door. The burner is fired with butane gas and is a high velocity burner with a heat release rate of 160.3 kW. It is 480 mm in length and is connected with an air/fuel regulator (Ighodalo and Ajuwa, 2006). The furnace chamber is mounted on a

tilting mechanism. The isometric view for the complete assembly of furnace components is as shown in Fig. 1.

Furance modeling: The model adopted is a one-dimensional model which consists of a governing equation for the combustion chamber and a transient heat conduction equation for the walls and roof. Each furnace component is treated as a one dimensional conduction medium and the governing equations are solved numerically to yield the gas, walls and roof temperature profiles which can be compared with experimental data. A similar one-dimensional model has been used by Bui and Perron (1988) and Davies *et al.* (2000). The components of the furnace for the purpose of modeling are as shown in Fig. 2.

Equations governing the combustion chamber: The furnace chamber is governed by an ordinary differential equation describing the conservation of energy of the gas body (Bui and Perron, 1988). It states that the rate of energy accumulation in the gas equals the heat brought into the gas by the combustion of the fuel, minus the sum of the heat transferred to the furnace structure (walls and roof), through chimney and into the melt:

$$V_7 C_{v7} \frac{dT_7}{dt} = Q_7 - \{Q_{71} + Q_{70} + Q_{72}\} \quad (1)$$

This equation is simply evaluated over time using a backward difference approximation. Q_7 is given by the combustion of natural gas:

$$Q_7 = \sum_{P} n_1 \int_{298}^{T_{out}} C_p\,(T)\,dT + \Delta H_{298} + \sum_{R} n_1 \int_{T_{in}}^{298} C_p\,(T)dT \quad (2)$$

Where P and R are the products and reactants. The combustion is assumed to be complete and stoichiometric. The constant pressure specific heat terms $c_p(T)$ are approximated using polynomials of temperature (T) of the form:

$$C_p\,(T) = a + b\times10^{-2}\,T + c\times10^{-5}T^2 + d\times10^{-9}T^3 \quad (3)$$

Where a, b, c and d are constants for each gas in the combustion product. Q_{71}, Q_{70} and Q_{72} are the heat flow through the walls, metal and extraction system, respectively as shown in Fig. 2. These are calculated using radiation and convection moldels.

The radiation and convection models: Radiosity approach is employed in modeling thermal radiation in the furnace chamber. The radiosity expression for each surface in an enclosure with combustion gas is as given by Davies *et al.* (2000):

$$Ji = \in i\, E_{bi} + \ell(\sum F_{ij}\tau g\, J_j) + \ell_i \in_g E_{bg} \quad (4)$$

Where:

$$\ell = 1 - \in_i, E_{bg}$$

is emisitivity of gas medium, τ_g is transmissivity of gas evaluated at the temperature of the jth wall:

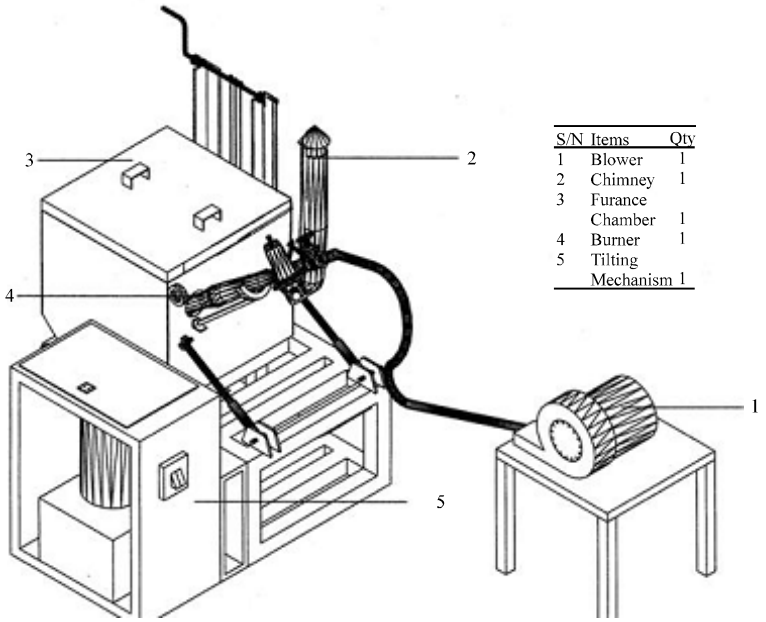

S/N	Items	Qty
1	Blower	1
2	Chimney	1
3	Furance Chamber	1
4	Burner	1
5	Tilting Mechanism	1

Fig. 1: Isometric view of the furnace

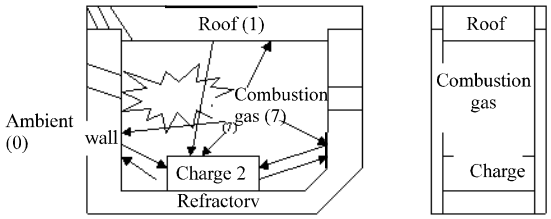

Fig. 2: Approximate representation of furnace chamber

$$Q_i = {}_i\frac{\varepsilon A_i}{1-\varepsilon}(E_{bi} - J_i) + hA_i(T_g - T_s) \tag{5}$$

The emissivity and absorptivity of the combustion gases used in Eq. 2 are obtained from the mixed grey gas model (Tucker, 2003):

$$\varepsilon_g(T_g) = \sum_n a_n(T_g)[1 - \exp(-K_{g,n} p L_m)] \quad \text{for } n = 1, N \tag{6}$$

$$\alpha_g(T_s) = \sum_n a_n(T_s)[1 - \exp(-K_{g,n} p L_m)] \quad \text{for } n = 1, N \tag{7}$$

and

$$\sum_n a_n(T_g) = 1 \text{ and } \sum_n a_n(T_s) = 1$$

Where:

a_n = The weighting coefficients

T_g and T_s = Gas and wall surface temperatures, respectively

$K_{g,n}$ = Absorption coefficient

L_m = The mean beam length which for a particular geometry can be approximated from (Holman, 1992)

$$L_m = 3.6 * \frac{V}{A} \tag{8}$$

Where, V is the total volume of the gas and A is the total surface area. The weighting coefficients are simply represented by (Tucker, 2003):

$$a_n(T_g) = b_{1,n} + b_{2,n} T_g \tag{9}$$

$$a_n(T_s) = b_{1,n} + b_{2,n} T_S \tag{10}$$

Where, $b_{1,n}$ and $b_{2,n}$ are constants. The radiation shape factors F_{ij} that are also needed in Eq. 4 were obtained from the expressions for two rectangles which are either parallel or at right angles were used. For parallel rectangles with equal sides of lengths a and b spaced a distance c apart, the edge distance ratios are X = a/c and Y=b/c. The view factor is given by Siegel and Howell (1972):

$$F_{ij} = \frac{2}{\pi XY}\left\{\ln\left[\frac{(1+X^2)(1+Y^2)}{1+X^2+Y^2}\right]^{\frac{1}{2}} + X\sqrt{1+Y^2}\tan^{-1}\frac{X}{\sqrt{1+Y^2}} + Y\sqrt{1+X^2}\tan^{-1}\frac{Y}{\sqrt{1+X^2}} - X\tan^{-1}X - Y\tan^{-1}Y\right\} \tag{11}$$

For two rectangles hl and lw at right angles with a common edge l, the length ratios are H = h/l and W = w/l. The view factor as given by Siegel and Howell (1972) is:

$$F_{ij} = \frac{1}{\pi W}\left\{W\tan^{-1}\frac{1}{W} + H\tan^{-1}\frac{1}{H} - \sqrt{H^2+W^2}\tan^{-1}\frac{1}{\sqrt{H^2+W^2}} + \frac{1}{4}\ln\left\{\left[\frac{(1+W^2)(1+H^2)}{(1+W^2+H^2)}\right]\left[\frac{W^2(1+W^2+H^2)}{(1+W^2)(W^2+H^2)}\right]^{W^2}\left[\frac{H^2(1+H^2+W^2)}{(1+H^2)(H^2+W^2)}\right]^{H^2}\right\}\right. \tag{12}$$

An estimate of the convective heat-transfer coefficient at the longitudinal walls was obtained from the expression:

$$h = 0.293G^{0.78} \tag{13}$$

The coefficient to the end walls were obtained from values reported for flow normal to a plate:

$$h = 0.023(t_k/d)Re^{0.8}\,Pr^{0.4} \tag{14}$$

Where t_k is the thermal conductivity for furnace gas, d is the hydraulic diameter for rectangular cross-section and is given by Rajput (1998):

$$d = \frac{4lb}{(2l+2b)} \tag{15}$$

With the heat flows so determined, Eq. 3 is evaluated over time using a backward difference approximation to yield the average gas temperature T_7. The stack gas

temperature T_{7s} can be obtained using the expression proposed by Hotel and Sarofim (1965) as given by Bui and Perron (1988):

$$T_{7g} = \frac{1}{6}T_{FA} + \frac{1}{3}T_E + \frac{1}{2}T_{7s} \quad (16)$$

where, T_{7g} is effective radiating temperature, T_{FA} is the adiabatic flame temperature, T_E is temperature of refractories surrounding the burner. The thermal efficiency is given by:

$$\eta_T = \frac{Q_7}{Q_{fuel}} \quad (17)$$

Equation governing the walls and roof: The heat transfer within the walls and roof is by conduction and each wall is treated as a one dimensional slab governed by the unsteady 1-D conduction equation (Sachdeva, 2008):

$$\frac{\partial T}{\partial t} = \alpha\frac{\partial^2 T}{\partial x^2}, 0 \le x \le L \quad (18)$$

Where the thermal diffusivity:

$$\alpha = k/\rho c$$

ρ = Density
c = The specific heat capacity
k = The thermal conductivity
T = The temperature

The body i.e., the wall is divided into a number of elements, the finite difference approximation is obtained for the governing equation and the appropriate form for internal and boundary nodes are established so that the temperature-time history can be obtained. The explicit form of the discretised equation for both internal and boundary nodes respectively are:

$$T_{i,j+1} = \frac{1}{R}(T_{i+1,j} + T_{i-1,j}) - T_{i,j}\left(\frac{1}{R} - 1\right) \quad (19)$$

where, $T_{i,J+1}$ is the temperature of an unknown mesh point (at time period j + 1) and it is now expressed in terms of the known temperatures on the previously calculated time period j:

$$Q_o.\frac{2\alpha\Delta t}{(\Delta x)^2}.\frac{\Delta x}{k} - \frac{\alpha\Delta t}{(\Delta x)^2}.2(T_0^n - T_1^n) = T_0^{n+1} - T_0^n \quad (20)$$

For convergence or stability of the numerical solution Δt and Δx should be chosen in such a manner that:

$$R = \frac{(\Delta x)^2}{\alpha \cdot \Delta t} \ge 2$$

Boundary and initial conditions: The initial condition for Eq. 1 is obtained by assuming that at the start of the simulation the gas body has previously reached a steady state and therefore the the accumulation term is nil:

$$V_7 C_{v7}\frac{dT_7}{dt} = 0$$

The boundary conditions for the walls and charge are of the known boundary heat flux type, as the radiation and convection heat fluxes are calculated separately. At the start of simulation all surfaces are assumed to be at ambient temperature. The initial condition is:

$$T_o = 30°C \quad \text{at } t = 0$$

The heat received by radiation and convection is conducted into the walls and charge so that the boundary condition is:

$$-k\frac{\partial T}{\partial x} = Q_{rad} + Q_{conv} \quad (21)$$

Model algorithm: A computer program written in MATLAB was developed based on the models presented. The flow chart for the simulation is shown in Fig. 3. For the given conditions of furnace geometry, fuel properties, furnace gas composition, charge and wall refractory

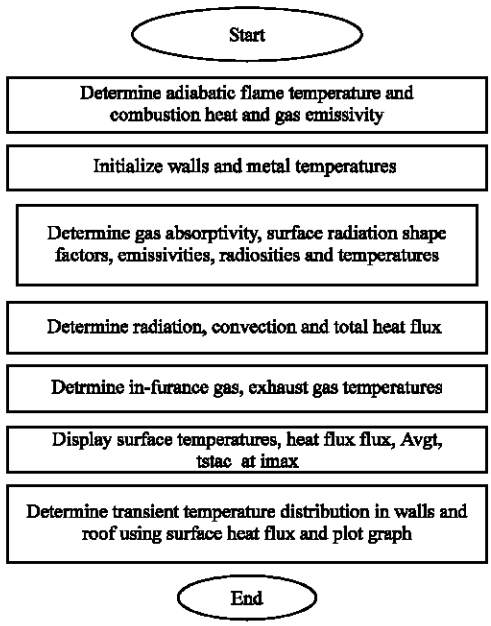

Fig. 3: Flowchart for computer program

properties, the adiabatic temperature and heat of gas combustion is estimated. The wall surface and charge surface temperature is initialized and the gas emissivity and absorptivity are calculated, shape factors for the surfaces are determined which leads to the determination of direct exchange areas. The radiosities for the surfaces are obtained by matrix inversion, convective heat transfer coefficients are calculated so that the total heat fluxes for the surfaces are determined. The average in-furnace gas temperature and stack (exhaust) gas temperature are calculated. The heat fluxes become the boundary conditions used for the determination of the transient temperature history for the walls which are then plotted.

RESULTS AND DISCUSSION

The model was tested for the case of furnace operation melting 3 kg of aluminium charge. From the output of the program the maximum temperatures obtained at the end of melting for walls and roof, in-furnace average gas temperature (avtg) and stack or exhaust gas were compiled and are compared with experimental values as shown in Table 1. The simulated total heat flux for walls, roof and metal charge are shown in Table 2. Temperature versus time plots for both experimental and simulated values measured at 88 mm depth of furnace walls and roof are shown in Fig. 4 and 5, respectively.

Simulated temperatures versus time was also plotted for the inside wall surface as shown in Fig. 6 and the simulated temperature distribution across thickness of walls is shown in Fig. 7. From the simulations conducted, higher values of wall temperatures were obtained when compared with experimental values as shown in Table 1. The average difference is 236.4°C for the inner wall surface temperatures.

The wall temperature simulations are observed to be closely coupled as shown in Fig. 4 and 5, this is a confirmation of a uniform temperature distribution within the furnace. The simulated and experimental temperature curves follow a very similar profile in all cases increasing linearly as can be seen from the Fig. 4-7 with the roof having the maximum temperature from Table 1. Nodal temperatures across the walls thicknesses also display an almost linear decreasing distribution as can be seen from Fig. 7.

Higher values for the in-furnace gas, exhaust gas and metal surface temperatures were also produced by the simulation. The discrepancies between experimental and simulated values can be attributed to air in-leakage into the furnace, experimental errors and simplifying

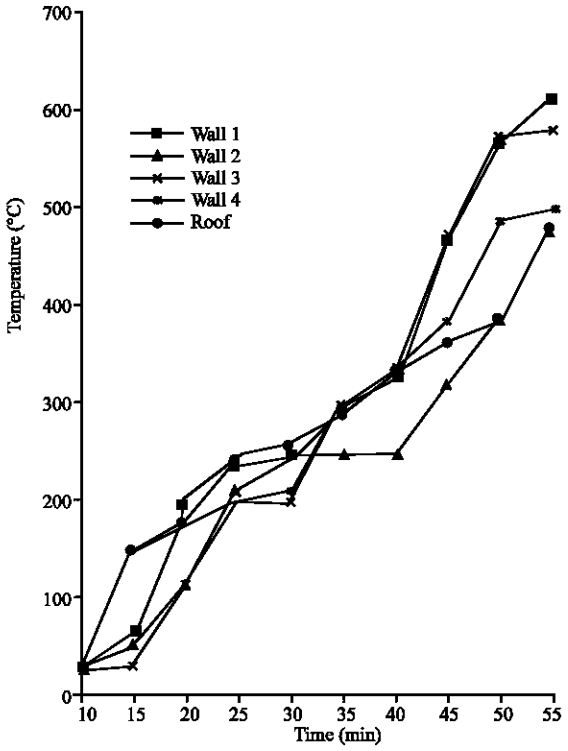

Fig. 4: Experiment temperature versus time plot (88 mm depth in furnace wall)

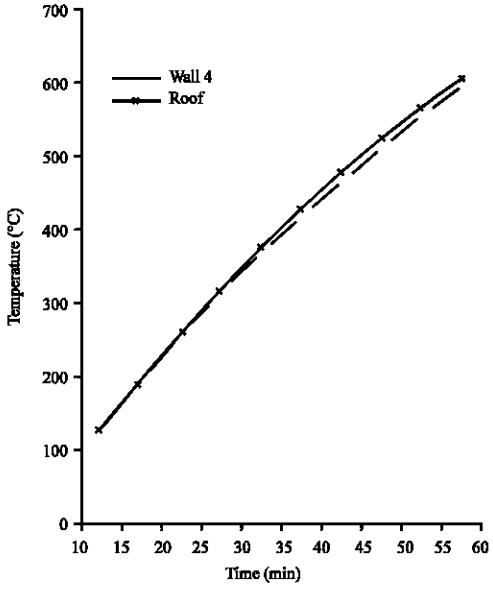

Fig. 5: Simulated temperatures versus time plot (88 mm depth in furnace walls)

assumptions employed in the simulations. The results obtained from the simulations can be said to be in fairly good agreement with the experimental values, thus

Table 1: Experimental and Simulated temperatures for walls, roof, in-furnace, exhaust gas and metal respectively in °C

Wall	Wall 1	Wall 2	Wall 3	Wall 4	Roof	Avtg	Tstac	Metal
Experiment	770.0	745.0	735.0	700.0	780.0	1025.0	593.8	660.0
Simulated	986.5	987.6	985.4	965.9	986.5	1692.4	833.0	756.9

Table 2: Simulated Total heat flux for walls, roof and metal

Wall	Wall 1	Wall 2	Wall 3	Wall 4	Roof	Metal
Heat flux (watts m^{-2})	21780	21828	21776	21333	21803	5529

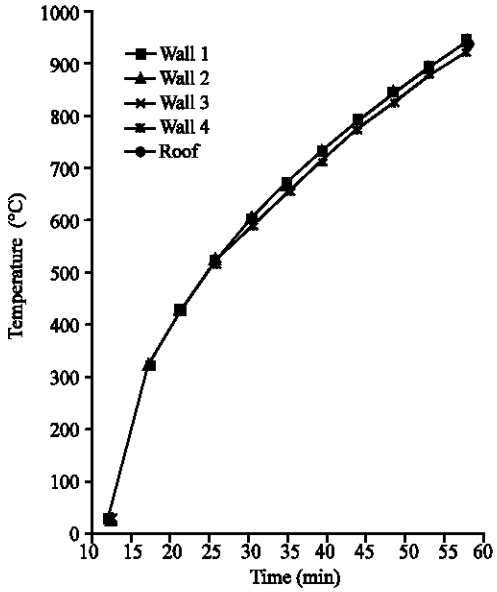

Fig. 6: Simulated inside wall surface temperature versus time plot

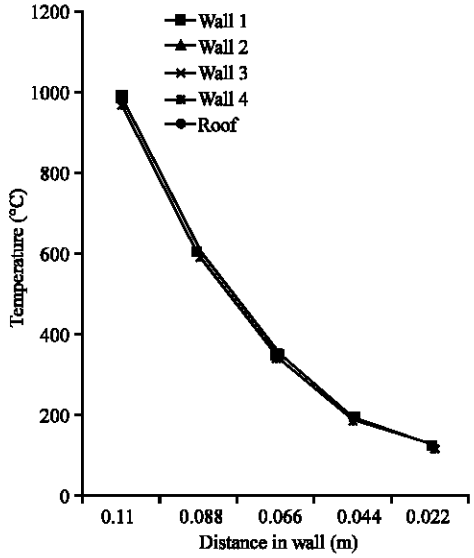

Fig. 7: Temperature range across wall thickness

validating the model employed. From Table 2, the heat fluxes to the walls are also observed to be uniform, all within 21 kW m^{-2}, this is not surprising since a uniform temperature obtains within the furnace. The heat flux on the metal charge is lower than for the walls and is adequate for melting of the charge. The thermal efficiency calculated by the model is 47.52%.

CONCLUSION

The one-dimensional model employed in modeling the furnace have produced results which are comparable with experimental data. From the foregoing the model is capable of predicting the key dependent variables, the average inside wall surface temperature, the net heat transfer rate to the exposed wall surfaces, the net heat transfer rates to the metal, the average in-furnace gas temperature and the metal surface temperature.

REFERENCES

Baukal, C.E. Jr., V.Y. Gershtein and X. Li, 2001. Computational Fluid Dynamics in Industrial Combustion. CRC Press, USA., pp: 630.

Bui, R.T. and J. Perron, 1988. Performance analysis of the aluminum casting furnace. Metallurgical Trans. B., 19: 171-180.

Davies, S.B., I. Master and D.J. Gethin, 2000. Numerical modeling of a rotary aluminum recycling furnace. Proceedings of the 4th International Symposium of Recycling of Metals and Engineered Materials, USA., pp: 1113-1121, http://Iweb.tms.org/Purchase/ProductDetaIl.aspx? Product_code=01-4941-1113.

Holman, J.P., 1992. Heat Transfer. 7th Edn., McGraw Hill Book Co., Singapore, pp: 713.

Hotel, H.C. and A.F. Sarofim, 1965. The effect of gas flow patterns on radiator transfer in cylindrical furnaces. Int. J. Heat Mass Transfer, 8: 1153-1169.

Ighodalo, O. and C.I. Ajuwa, 2006. Development and performance evaluation of a high velocity burner. J. Applied Basic Sci., 4: 133-138.

Ighodalo, O.A. and C.I. Ajuwa, 2010. Development and performance evaluation of a melting furnace for non-ferrous metals. Int. J. Eng., 4: 57-64.

Khalil, E.E., 1982. Modeling of Furnaces and Combustors. Abacus Press, UK., pp: 260.

Rajput, R.P., 1998. A Textbook of Fluid Mechanics. Chand and Company Ltd., India, pp: 876.

Sachdeva, R.C., 2008. Fundamentals of Engineering Heat and Mass Transfer. 3rd Edn., New Age International Ltd., New Delhi, pp: 684.

Siegel, R. and J.R. Howell, 1972. Thermal Radiation Heat Transfer. McGraw-Hill Inc., New York, pp: 814.

Szekely, J., 1988. The mathematical modeling revolution in extractive metallurgy. Metallurgical Trans., 19: 525-540.

Tucker, R.J., 2003. Gas emissivity. Zerontec Ltd. btinternet.com/~robertjtucker/gas_emissivity.htm.